

**Resonant fluorescence line narrowing measurements in erbium-doped glasses for optical amplifiers**

Laurent Bigot,\* Anne-Marie Jurdyc, and Bernard Jacquier

*Laboratoire de Physico-Chimie des Matériaux Luminescents, Université Lyon 1, UMR-CNRS 5620, 10 rue André-Marie Ampère, Campus de la Doua, 69622 Villeurbanne Cedex, France*

Laurent Gasca and Dominique Bayart

*Alcatel Research and Innovation Department, Route de Nozay, 91461 Marcoussis, France*

(Received 19 March 2002; published 11 December 2002)

Rapid development of optical fiber amplifiers, and more especially of the erbium-doped fiber amplifiers (EDFA) during the last decade, has benefited from extensive work on the configuration of the system itself: determination of pump wavelength, pumping configuration, improvement of noise performance, etc. However, less effort have been dedicated to study the interaction that influences the spectral profile of the gain bandwidth and particularly the relation between the glass composition and the spectroscopy of erbium. Here, we report a systematic determination of key parameters responsible for the global profile of the gain bandwidth: stark splitting, homogeneous broadening, and inhomogeneous broadening. The correlation between these parameters and the glass structure from one part and the behavior of the EDFA in amplification regime from another part is discussed. The quasiregular crystal-field splitting of tellurite and fluoride glasses is found to correlate well with the flatness of the gain profile. Moreover, the low-temperature homogeneous bandwidths extrapolated to room temperature can be correlated to the saturation spectral hole widths measured in the amplification regime.

DOI: 10.1103/PhysRevB.66.214204

PACS number(s): 32.50.+d, 32.70.-n, 39.30.+w, 78.20.-e

**I. INTRODUCTION**

The advent of optical fibers during the 1980s and of optical fiber amplifiers during the 1990s permitted a continuous evolution of telecommunications leading to the Internet revolution of the last few years. As a consequence of the development of the wavelength division multiplexing (WDM) technology associated to the erbium-doped fiber amplifiers (EDFA's) for the third telecommunication window around 1.55  $\mu\text{m}$  (references in Ref. 1), the volume of data transported has doubled during the last two years.<sup>2</sup> In the next few years, however, the information carrying capacity will have to increase by several orders of magnitude. Strategies considered for the future are the following:

- Development of new amplification bands that requires the use of new doped materials. A possible candidate is the S band exhibited by thulium, which permits amplification of signals around 1.5  $\mu\text{m}$ .<sup>3,4</sup>
- Reduction of the spacing between the channels that transport information. At present, the typical spacing is around 100 GHz but many workers are already exploring spacings of 50 GHz or less (DWDM: dense wavelength division multiplexing).<sup>5</sup>
- Broadening of the C band (1530–1560 nm) and L band (1570–1600 nm) of EDFA's. In the case of the L band, new hosts like modified silicate could extend the amplification range to longer wavelengths.<sup>6</sup>

The last two solutions require improved gain characteristics (width, flatness) of the present EDFA's. That requires a better understanding of the key parameters determining those characteristics, namely, Stark splitting, homogeneous broadening, and inhomogeneous broadening of the transitions involved.

In the past, some linewidth broadening studies have been performed on erbium ions in glassy hosts<sup>7,8</sup> and also in the amplification regime<sup>9,10</sup> or using broadening extrapolated from direct deconvolution of the whole emission/absorption spectra.<sup>11</sup> The last approach can, in better cases, only give a rough idea of the broadening values, so the first one is much more interesting because it involves the direct measurement of the homogeneous broadening. Measurements in the amplification regime are quite an unusual approach that determines homogeneous broadening by studying the gain saturation. So, it is interesting to compare it to a conventional high-resolution spectroscopy approach like fluorescence line narrowing (FLN) or spectral hole burning (SHB) experiments.

In the case of Stark splitting measurements, though deconvolution of room-temperature spectra<sup>11</sup> was proposed, many workers are using low-temperature measurements to more clearly isolate each energy level.<sup>12–15</sup> Recent studies have succeeded in giving the position of all the Stark levels of most of the manifolds of erbium ion;<sup>16,17</sup> however, there is a need for more results, especially in very different hosts.

Actually, as in the case of linewidth measurements, the need for exact energy-level values comes from a lack of knowledge about glass structure. Indeed, it is still nearly impossible to predict the influence of a given glass composition on the spectroscopy of a rare-earth ion. The aim of this work is therefore to make the first systematic determination of Stark splitting, homogeneous broadening, and inhomogeneous broadening in four very different hosts using high-resolution spectroscopy, namely resonant fluorescence line narrowing (RFLN). Comparing the different parameters obtained, it is then possible to project their dependence on the glass structure and also their influence on the erbium gain spectrum.

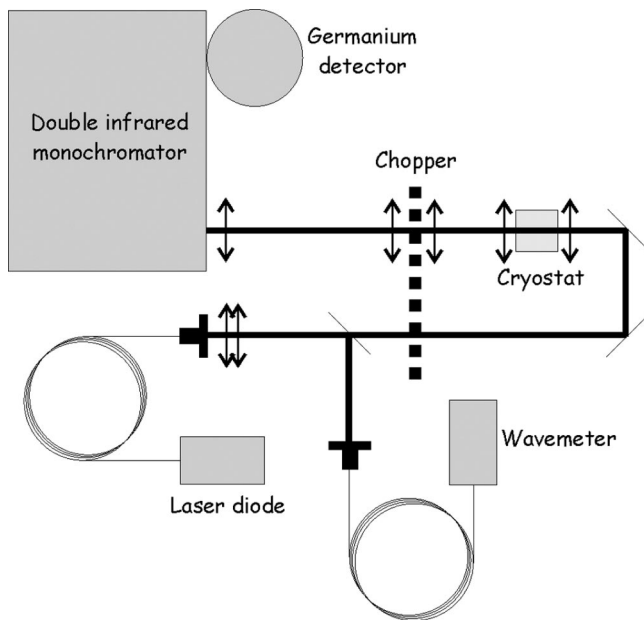


FIG. 1. Experimental setup used for resonant fluorescence line narrowing experiments. See the text for other information.

After a short description of the experimental setup used for our experiments, we will present the results obtained, giving the general trends observed. Several questions will then be discussed:

- the relation between the Stark splitting and the glass composition;
- the evolution of the inhomogeneous broadening from one glass to another and how it can be related to what is known about the glass structure;
- the influence of the matrix on the homogeneous broadening.

This last point will be especially discussed in terms of the temperature dependence of the homogeneous linewidth. We also show that these measurements can be correlated to measurements made in the amplification regime. This shows that our measured parameters give information on the gain bandwidth of the amplifier.

## II. EXPERIMENT

Three different kinds of high-resolution spectroscopy experiments were carried out: emission at low temperature, site-selective spectroscopy, and RFLN. The experimental setup is the same for all the measurements and is shown in Fig. 1. The sample was excited using a spectrally narrow and tunable laser diode. The typical linewidth of the laser is 50 MHz in the 1480–1580 nm wavelength range for the time scale of the emission spectrum. The laser power is less than 5 mW and the beam waist is around 300  $\mu\text{m}$ . We checked that this power density is low enough to avoid power broadening. The sample was mounted in a liquid-helium bath cryostat that enables measurements in the temperature range of 1.5–300 K. The luminescence emitted by the sample was collected in the forward direction and focused onto the en-

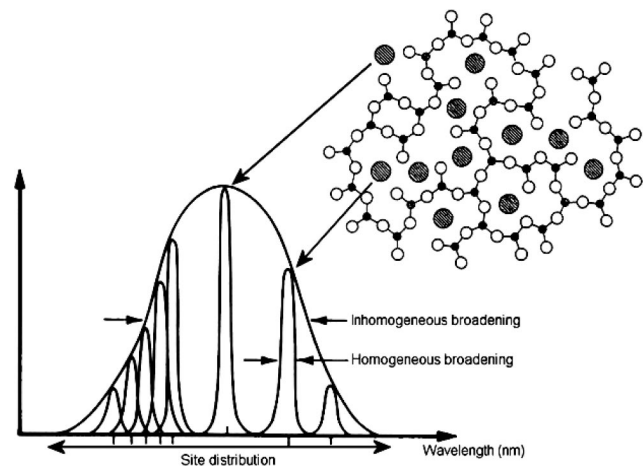


FIG. 2. Schematic drawing of the homogeneous broadening, inhomogeneous broadening, and site distribution. Each erbium ion possesses its own spectroscopic signature, giving access to the homogeneous broadening. The shape of all the individual contributions leads to inhomogeneous broadening.

trance slit of a 1-m Jobin-Yvon U1000 infrared monochromator. The signal was then detected by a high-sensitivity germanium-cooled detector from North Coast. A chopper was used to modulate the incoming laser beam and modulate out of phase the fluorescence and the output laser beam.<sup>7</sup> This eliminates the laser light before it reaches the monochromator and permits recording of the fluorescence at the same wavelength as the laser excitation with a delay of about 1 ms, small compared to the long lifetime of the 1.55- $\mu\text{m}$  emission of erbium. It also allows amplification of the signal using a lock-in amplifier. The investigated samples were preforms or bulk samples of aluminosilicate, alkalisilicate, fluoride, and tellurite erbium-doped glasses. All the samples contained 0.1 wt % of erbium (except the fluoride sample used for inhomogeneous broadening measurements which contains 1 wt % of erbium and the alkalisilicate which contains 0.4 wt % of erbium). Three experiments were carried out:

Emission at low temperature: Emission at 1.5 K with non-selective excitation into the  $^4I_{13/2}$  level determines the average  $^4I_{15/2}$  Stark splitting. To obtain information on the  $^4I_{13/2}$  level, the  $^4S_{3/2}$  level was excited at 1.5 K using an Argon laser line and the  $^4S_{3/2} \rightarrow ^4I_{13/2}$  emission was detected with a 60-cm Jobin-Yvon HRS1 visible monochromator with a GaAs photomultiplier.

Site-selective spectroscopy: A given site was excited in the first excited state and its fluorescence collected at 1.5 K. Changing the laser wavelength probed another site and allowed to reach the Stark splitting of the specific site. The reconstruction of the site distribution was obtained by recording the intensity of the fluorescence at the same wavelength as the excitation for each excitation wavelength. A plot of these measured intensities with laser wavelength is representative of the inhomogeneous broadening which corresponds to the full width at half maximum (FWHM) of the linewidth.

RFLN: Fluorescence at the same wavelength as the excitation wavelength in the temperature range 30–150 K indicates the zero-phonon transition (transition between the low-

est levels of the  $^4I_{13/2}$  and  $^4I_{15/2}$  manifolds) and its linewidth (FWHM of the linewidth) is proportional to the homogeneous broadening.

### III. THEORY

*Stark splitting.* In rare earth ions, the energy levels are influenced by the nature of the matrix that surrounds the ion and acts as a perturbation on the energy levels of the free ion. When such an ion is embedded in a host (crystal or glass), it experiences an electric potential that has the same symmetry as the crystallographic site. The splitting of the free ion manifolds leads to Stark levels. The degree of the degeneracy remaining depends on the symmetry of the site: the higher the symmetry, the higher the degree of degeneracy. In a glassy host, the symmetry is assumed to be very low and therefore the manifolds are fully split.<sup>18</sup> For erbium, each manifold is composed of  $J + \frac{1}{2}$  Stark levels. For larger crystal field, larger Stark splitting of the  $^4I_{15/2}$  and  $^4I_{13/2}$  manifolds occurs; the relative positions of the Stark levels to the barycenter of the manifolds indicate deviation from spherical symmetry.

*Broadening of the energy levels.* The broadening of the Stark levels has two origins: a homogeneous broadening that is related to a given ion in the matrix and an inhomogeneous broadening that is the global distribution of all the homogeneous contributions, as can be seen in Fig. 2:

- Homogeneous broadening: There are many contributions to the homogeneous broadening at high temperature: direct phonon processes, two-phonon processes (Raman and Orbach processes, for example), and both multiphonon and radiative relaxations. All these processes lead to Lorentzian line shapes and will be detailed hereafter.
- Inhomogeneous broadening: In the case of a glassy host, this broadening is related to the existence of many different sites for the ions. It is commonly assumed that this broadening results in a Gaussian line shape. For glasses, this broadening (the FWHM of the Gaussian line shape) is around hundreds of wave numbers ( $\text{cm}^{-1}$ ), that is to say about 1000 times larger than in crystals where the environment is much more uniform.

Hence the width of a transition between two Stark levels may be written as

$$\Delta E(T) = E_{\text{inhomogeneous}} + \underbrace{E(T)_{\text{direct}} + E(T)_{\text{Raman}} + E(T)_{\text{multiphonon}} + E_{\text{radiative}}}_{E_{\text{Homogeneous}}}. \quad (1)$$

- Direct process:

$$\begin{aligned} \Delta E(T)_{\text{Direct}} &= \Delta E(T)_{\text{Direct}}^{\text{Emission}} + \Delta E(T)_{\text{Direct}}^{\text{Absorption}} \\ &= \sum_{j < i} \beta_{ij} \left( \frac{1}{e^{\Delta E_{ij}/kT} - 1} + 1 \right) \\ &\quad + \sum_{j < i} \beta_{ij} \left( \frac{1}{e^{\Delta E_{ij}/kT} - 1} \right). \end{aligned} \quad (2)$$

In Eq. (2),  $i$  and  $j$  are two Stark levels with an energy difference  $\Delta E_{ij}$ .  $\beta_{ij}$  are the coupling coefficients for the ion-phonon interaction. In this case, a single phonon is emitted or absorbed. These processes have to be taken into account for the excited state and for the ground state. When the energy separation between the two levels is beyond the range of phonon energies, a direct process can still occur via multiphonon relaxation.

- Raman process:

$$\Delta E(T)_{\text{Raman}} = \alpha \left( \frac{T}{T_D} \right)^7 \int_0^{T_D/T} \frac{x^6 e^x}{(e^x - 1)^2} dx, \quad (3)$$

where  $\alpha$  is the coupling coefficient for the ion-phonon interaction and  $T_D$  is the effective Debye temperature of the phonon distribution. The Debye temperature is related to

the phonon cutoff frequency via

$$T_D = \frac{\hbar \omega_D}{k}. \quad (4)$$

In the Raman relaxation process, the system first “absorbs” a phonon which promotes it in a virtual energy level. Then, it relaxes “emitting” a second higher energy phonon. The same process can occur involving a real energy level and is called an Orbach process. The energy of the phonons involved in these two processes is in the range of the phonon energies of the system, which implies that the energy levels involved are the crystal levels of the same manifold. The value of integral in Eq. (3) has been tabulated by Di Bartolo.<sup>19</sup> This contribution is proportional to  $T^7$  at low temperature ( $< 20$  K typically) and  $T^2$  at high temperature ( $> 100$  K typically). It is generally found that the Debye temperature used in Eq. (3) is lower than the Debye temperature determined using Eq. (4).<sup>20</sup> This can be explained by the fact that, at low energy, the density of energy phonon states is higher than that predicted by the Debye theory.

- Radiative processes:

According to the Heisenberg principle and due to the long relaxation times of the intra- $4f^n$  transitions (some microseconds to milliseconds), these processes are assumed to be negligible compared to the previous ones.

TABLE I. Positions of the Stark levels of the  $^4I_{15/2}$  manifold derived from low-temperature  $^4I_{13/2} \rightarrow ^4I_{15/2}$  emission spectra for the different glasses studied in this work (illustration in Fig. 6). The positions are given with respect to the first Stark level.

	Aluminosilicate ( $\text{cm}^{-1}$ )	Alkalisilicate ( $\text{cm}^{-1}$ )	Fluoride ( $\text{cm}^{-1}$ )	Tellurite ( $\text{cm}^{-1}$ )
Z1	0	0	0	0
Z2	26.9	23.4	18.3	22
Z3	45.4	32.9	34.3	41.4
Z4	71.6	53.9	50.1	56.4
Z5	92.9	95.7	115.4	106.5
Z6	136.4	114	190.3	198.1
Z7	222.6	389.3	236.5	245.7
Z8	330.3	467.1	314.4	310.3

For the lowest Stark level of a given manifold, it is commonly assumed that the contribution to the total linewidth of multiphonon relaxation can be neglected because of the large energy gap between the manifolds involved. The contribution of Raman and direct processes varies with the temperature: meanwhile the linewidth at low temperature is mainly caused by direct one-phonon process, the Raman-scattering processes may become dominant at high temperature. Since upper Stark levels are separated from the lowest one by energies of tens to several hundreds of wave numbers, which fits the typical phonon energy, the direct process and in particular spontaneous emission, should be the dominant process for these levels.<sup>21</sup>

#### IV. RESULTS AND COMMENTS

*Stark splitting.* Stark splittings of the  $^4I_{15/2}$  level are collected in Table I. Assuming a completely removed degeneracy of the  $^4I_{15/2}$  manifold, the positions have been obtained by deconvolution of the  $^4I_{13/2} \rightarrow ^4I_{15/2}$  emission recorded at low temperature into eight Gaussian-type profiles. The reported position for each level of the  $^4I_{15/2}$  manifold is the

TABLE II. Positions of the Stark levels of the  $^4I_{13/2}$  manifold derived from low-temperature nonresonant emission spectra (spectra not reported here). The positions are given with respect to the first Stark level.

	Aluminosilicate ( $\text{cm}^{-1}$ )	Alkalisilicate ( $\text{cm}^{-1}$ )	Fluoride ( $\text{cm}^{-1}$ )	Tellurite ( $\text{cm}^{-1}$ )
Y1	0	0	0	0
Y2		39	27.1	48.9
Y3		80.2	77	78.2
Y4		101.6	110.6	104.5
Y5			140.3	138
Y6		$\geq 270$	197.1	182.4
Y7			249.3	221.4

mean value over the whole site distribution. A full deconvolution of the first manifold has been performed for all the tested hosts and is shown in Fig. 3. Note that, in the case of aluminosilicate, the position of the last two levels does not appear as clearly as in the other glasses due to a strong overlap of the Stark levels. Splittings for the  $^4I_{13/2}$  are given in Table II. A full deconvolution of this manifold has only been performed in two of the four tested hosts. All the splittings obtained in this work are compared to previous results in Table III. This is a systematic comparison of four very different matrices.

*Inhomogeneous broadening.* As is shown in Fig. 4, the inhomogeneous broadening is determined by the fit into Gaussian-type profiles of the maximum intensities of the zero-phonon transition of different sites. Each individual measurement was obtained within conditions as rigorously identical as possible. The inhomogeneous broadening is the FWHM of the Gaussian distribution. One can note that, in all cases, a single Gaussian line shape was obtained that fits very well the emission spectrum recorded under nonselective excitation (at higher energy than the zero-phonon transition). This approach is quite original; indeed, deconvolution of low-temperature absorption spectrum is generally used to de-

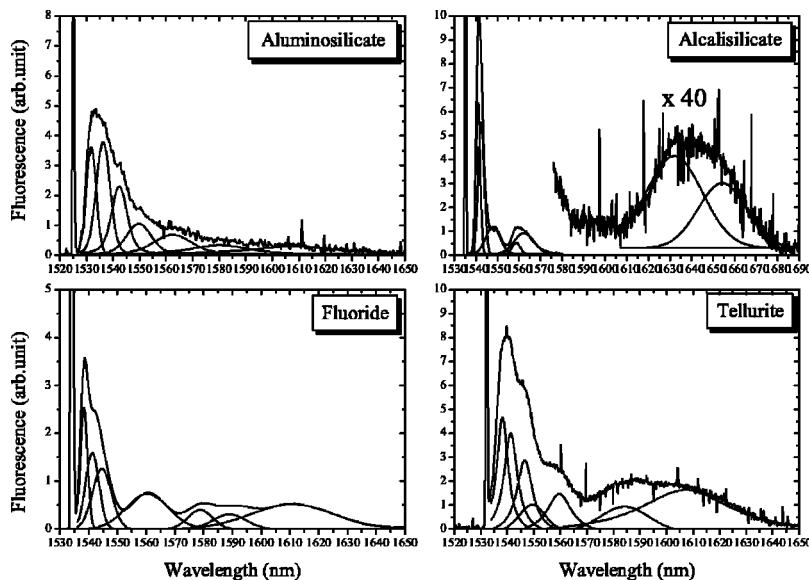


FIG. 3.  $^4I_{13/2} \rightarrow ^4I_{15/2}$  emission for the different glass compositions at 1.5 K. In each case, deconvolution of the spectrum is also reported. This enables the determination of the eight Stark levels of the  $^4I_{15/2}$  manifold.



TABLE III. Position of the Stark levels of the  $^4I_{15/2}$  and  $^4I_{13/2}$  manifolds (from literature). For each manifold, the positions are given with respect to the first Stark level.

	Phosphate (Ref. 12) ( $\text{cm}^{-1}$ )	Silicate (Ref. 16) ( $\text{cm}^{-1}$ )	Germanate (Ref. 16) ( $\text{cm}^{-1}$ )	Fluoride (Ref. 17) ( $\text{cm}^{-1}$ )
Z1	0	0	0	0
Z2	26	23	35	47
Z3	62	50	63	111
Z4	107	70	82	154
Z5	220	139	108	194
Z6	390	295	274	226
Z7	440	386	377	275
Z8	500	443	457	341
	(6515)	(6498)	(6488)	(6542)
Y1	0	0	0	0
Y2	33	5	12	27
Y3	51	42	42	61
Y4	75	61	76	89
Y5	230	84	107	135
Y6	280	262	231	173
Y7	330	322	300	238

termine inhomogeneous broadening which implies to extract the site distribution from all the other transitions.

*Homogeneous broadening.* The homogeneous broadening is given by the deconvolution of the shape of the zero-phonon transition into Voigt-type profiles. An example of such a deconvolution is shown in Fig. 5 in the case of the fluoride glass. The Gaussian contribution to the Voigt profile corresponds to the spectral response of our detection system and the Lorentzian contribution is the homogeneous contribution. The Gaussian contribution was obtained by recording the spectrally narrow laser light directly with all the slits of the monochromator fixed at the same values as the ones used during the fluorescence measurements and corresponds to a resolution of around  $0.8 \text{ cm}^{-1}$ . The value of the homoge-

neous broadening is half the FWHM of the Lorentzian contribution as commonly assumed in the case of RFLN measurements.<sup>22</sup> For fluoride glass, it was also possible to estimate the homogeneous broadening of transitions involving upper Stark levels. For example, we can estimate the broadening of the  $Y_1 \rightarrow Z_5, Z_6, Z_7, Z_8$  transitions by deconvolution of the whole spectrum into eight Voigt-type profiles using, for each transition, the previously determined inhomogeneous broadening and peak position values; the homogeneous broadening is the free parameter of this deconvolution.

## V. DISCUSSION

In this section, we discuss the comparison of the different spectral parameters determined above for the different hosts

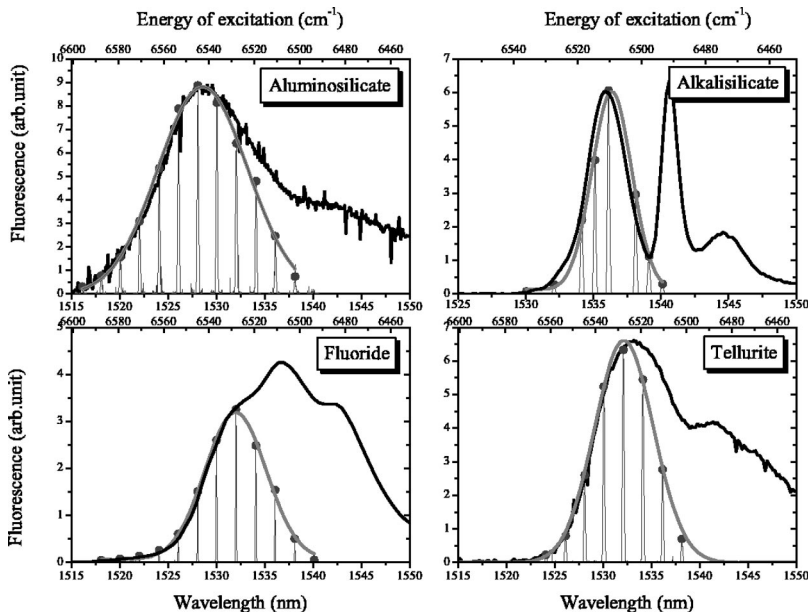


FIG. 4. Reconstruction of the inhomogeneous profile using site-selective spectroscopy: each individual point reports the maximum intensity of a resonant site selective emission spectrum. The envelop is the Gaussian fit (see the text). The full line is the nonresonant emission spectrum.

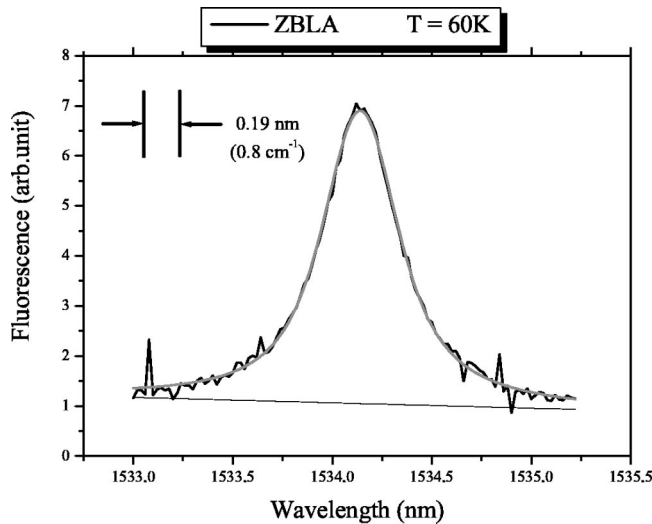


FIG. 5. Example of an experimental linewidth and of a fit of the zero-phonon transition using Voigt-type profile in the case of fluoride glass at 60 K. The resolution of our detection system is indicated in the inset.

and their incidence on the spectral properties of the EDFA.

**Stark splitting.** The  $^4I_{13/2}$  splitting is very similar, and typically a bit smaller than the  $^4I_{15/2}$  splitting; this is not very surprising because of the similar electronic nature ( $4f$  levels) of the two manifolds which have similar coupling with the surrounding matrix. The splitting is much larger for the  $^4I_{15/2}$  manifold in the case of aluminosilicate glass compared to the other glasses (Fig. 6). As explained before, this observation may be related to a higher crystal-field in the aluminosilicate glass composition. Two Stark levels are clearly far from the barycenter, which confirms that the symmetry may not be as low as is commonly assumed in glasses. These observations are in agreement with the conclusions of previous work based on a crystal field calculation approach.<sup>16,17</sup> Another interesting observation is the fact that, in fluoride glasses, the

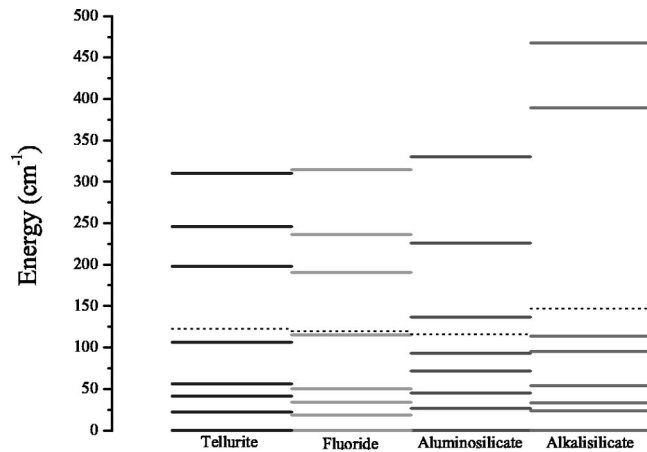


FIG. 6. Comparison of the Stark splittings of the  $^4I_{15/2}$  manifold for the different hosts with respect to the zero-phonon transition. The dotted line figures out the position of the barycenter of the manifold for each host. The energy levels correspond to the position of the Gaussian shapes obtained in Fig. 3.

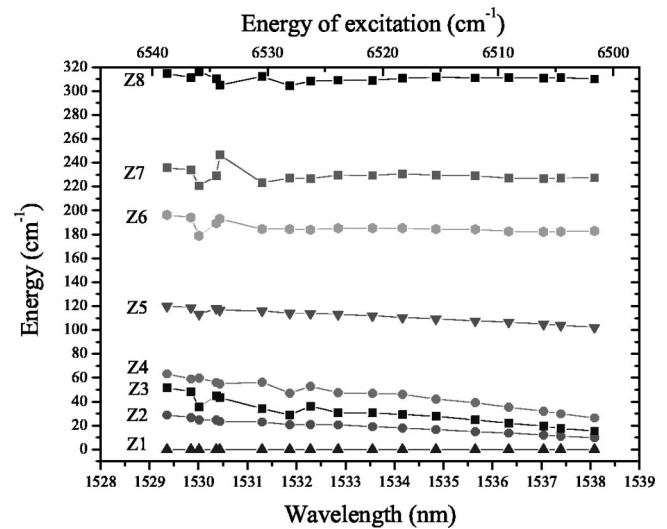


FIG. 7. Evolution of the positions of the Stark levels of the  $^4I_{15/2}$  manifold as a function of the energy of excitation for the fluoride sample with respect to the zero-phonon transition.

splitting is rather regular from one site to another as can be seen in Fig. 7. This point will be discussed later. The results also indicate that fluoride glasses exhibit, together with tellurite glasses, a quite regular spacing between the Stark levels which correlates with the flat gain obtained in the  $C$  band with these glasses.<sup>23</sup>

**Inhomogeneous broadening.** Associated with the small variation of the Stark splitting from one ion to another (see Fig. 7 in the case of the fluoride glass), the Gaussian shape obtained for all the matrices suggests that all the ions are located in similar sites, only slightly deformed from one ion to another. We clearly see that the inhomogeneous broadening is larger for aluminosilicate, fluoride, and tellurite than for aluminosilicate (see Fig. 4 and Table IV). If we compare aluminosilicate and aluminosilicate glasses, this trend can be explained by the fact that alkaline ions permit a better incorporation of rare-earth ions (high rare-earth doping concentrations are accessible<sup>24</sup>) in a more uniform environment: alkaline ions increase the solubility of the rare-earth ions in the silica network and decrease the rigidity of this network which apparently enables a smooth change of the symmetry from one ion to another.

**Homogeneous Broadening.** As is shown in Fig. 8, measurements of the homogeneous broadening at 120 K clearly exhibit different values for the four considered hosts with larger FWHM in the fluoride and tellurite than in aluminosilicate and aluminosilicate. The experimental temperature dependence of the homogeneous linewidth over the temperature range 30–150 K is around  $T^{1.5}$  for all the glass compositions (Table IV). This temperature law clearly indicates that both direct process (which leads to  $T^1$  temperature dependence) and Raman process (which leads to  $T^2$  temperature dependence) have to be taken into account. Very similar results of the temperature dependence have been previously obtained in amplification regime<sup>9,10</sup> though the homogeneous broadening value is smaller in our case. These observations are different from those reported in the literature that rarely

TABLE IV. Temperature dependence law of the homogeneous broadening. Inhomogeneous broadening FWHM and homogeneous broadening FWHM of the zero-phonon transition extrapolated at room temperature are also reported for all different hosts.

	Aluminosilicate	Alkalisilicate	Fluoride	Tellurite
Temperature dependence	$\sim T^{1.39 \pm 0.04}$	$\sim T^{1.42 \pm 0.13}$	$\sim T^{1.53 \pm 0.12}$	$\sim T^{1.7 \pm 0.13}$
Inhomogeneous broadening ( $\text{cm}^{-1}$ )	39.7	12.4	27	30.7
Homogeneous broadening ( $\text{cm}^{-1}$ )	8.7	7.1	11.3	13.5

deviates from a quadratic law for other rare-earth ions.<sup>25</sup> This difference is explained by the fact that:

- The splittings obtained indicate that the crystal levels are close from one to another: the mean spacing between the two first Stark levels of a manifold is around  $25 \text{ cm}^{-1}$ . However, the work reporting quadratic laws correspond to studies on europium, neodymium, and praseodymium ions for which the spacing is larger.
- The temperature range we have studied in this work is small compared to that of other works which include measurements at high temperature (200 K or above). This experimental fact results from the specific case of the  $1.55 \mu\text{m}$  erbium emission for which a strong overlap of all the transitions between ground and excited crystal-field levels beyond 150 K makes it difficult to extract the contribution of the zero-phonon transition. Nevertheless, it is expected that Raman process becomes dominant at high temperature, when  $T \approx T_D$ . Hence, in our case, we are still in a temperature range where there is a competition between Raman process and direct process.

Hence in the case of erbium, it is necessary to consider both Raman process and direct processes. To illustrate this point, the temperature dependence was fitted using the following analytical form of the broadening of the transition between the lower levels of each manifold:

$$\Delta E(T) = E_0 + \beta_1 \frac{1}{e^{\Delta E_1/kT} - 1} + \beta_2 \frac{1}{e^{\Delta E_2/kT} - 1} + \alpha \left( \frac{T}{T_D} \right)^7 \int_0^{T_D/T} \frac{x^6 e^x}{(e^x - 1)^2} dx. \quad (5)$$

In Eq. (5),  $\Delta E_1$  and  $\Delta E_2$  are the energy differences between the first and second Stark levels of the  $^4I_{15/2}$  and  $^4I_{13/2}$  manifolds.  $\beta_1$  and  $\beta_2$  are the coupling coefficients for the ion-phonon interaction for these two manifolds.  $E_0$  is the residual width for the two levels. Such an equation implies that:

- radiative and multiphonon processes are neglected;
- Raman process is considered to be the major two-phonon process and the Orbach process is neglected;
- phonon absorption between the lowest and the second Stark level is assumed to be the major contribution to the direct process.

The experimental temperature dependence of the FWHM were reproduced with a satisfactory agreement using Eq. (5), as can be seen in Fig. 8. All the parameters involved are reported in Table V and one can note that:

- the order of magnitude for all parameters is typical for rare-earth materials (comparison only with available data of crystals),<sup>26,27</sup>

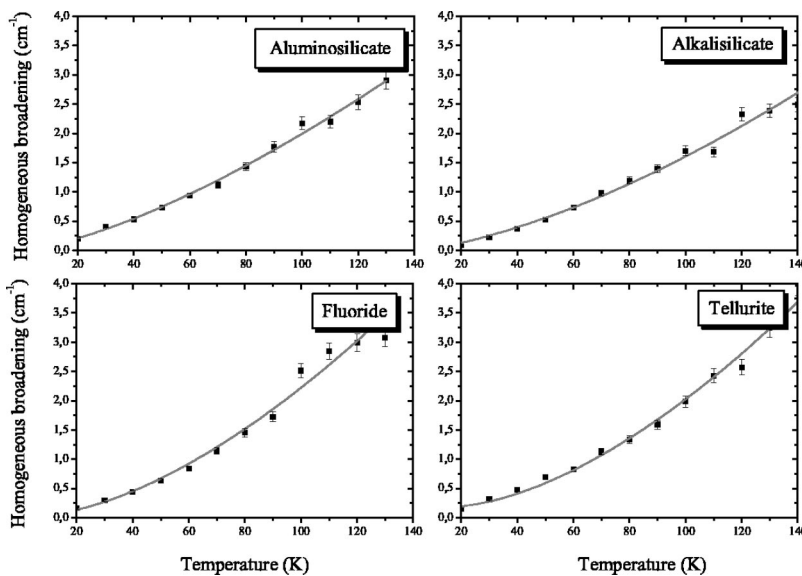


FIG. 8. Temperature dependence of the homogeneous broadening of the zero-phonon transition for the different glasses: the points are the measured widths and the lines correspond to the equation involving Raman and direct processes [see Eq. (5)].

TABLE V. Fitting parameters of Eq. (5) used to reproduce the temperature dependence of the homogeneous broadening using Raman and direct processes. The homogeneous broadening extrapolated using these parameters is also reported.

	Aluminosilicate	Alkalisilicate	Fluoride	Tellurite
$\alpha$ (cm <sup>-1</sup> )	18.3	15.6	17.6	25
$\beta_1$ (cm <sup>-1</sup> )	0.6	0.1	0.2	0.3
$\beta_2$ (cm <sup>-1</sup> )	0.2	0.8	0.1	0.5
$T_D$ (K)	292	300	163.2	224.9
$E_0$ (cm <sup>-1</sup> )	0.1	0	0	0
Homogeneous broadening at $T=300$ K (cm <sup>-1</sup> )	9.5	8.1	15.2	13.2

- the Debye temperature follows the same variation as the maximum phonon energy of the hosts studied: it is larger in aluminosilicate and alkalisilicate than in tellurite and fluoride.

For the transitions  $Y_1 \rightarrow Z_5, Z_6, Z_7, Z_8$  (see Fig. 9 in the case of fluoride glass), the observed temperature dependence is approximately linear over the temperature range studied. This emphasizes that the direct process is dominant for transitions involving upper Stark levels over a wide temperature range. This study was only possible in fluoride glass where the overlap between the different transitions is weak, which allows each level to be clearly distinguished.

Another interesting feature is to compare the results obtained in this work with those deduced from gain spectral hole burning (GSHB) experiments made earlier on two kinds of EDFA.<sup>28,29</sup> A GSHB experiment is a measurement of the spectral distribution of the gain in an amplification regime. With constant pumping conditions of the EDFA, a first spectral distribution of the gain is measured with a saturating signal wavelength. Then, the same measurement is performed without the saturating signal. The difference between

the two gain profiles underlines the local gain variation due to inhomogeneous gain behavior. The GSHB is studied more and more in the case of optical amplifiers, to predict this phenomenon which is very limiting in the case of submarine applications where amplifiers are cascaded, leading to huge gain variations. A few years ago, it was suggested that the hole width could be related to the homogeneous broadening.<sup>9,10</sup> This is confirmed by the theoretical study of gain saturation in the case of an inhomogeneous line shape which indicates that the hole corresponding to the local saturation has a FWHM equal to the homogeneous linewidth at high saturating intensities.<sup>30</sup> While the homogeneous broadening linewidths measured in this work are not equal to the hole FWHM reported for GSHB measurements,<sup>28,29</sup> it appears that:

- like the hole FWHM in GSHB measurements, the homogeneous broadening in fluoride glasses is twice the homogeneous broadening in aluminosilicate glasses;
- like the hole FWHM in GSHB measurements, the homogeneous broadening increases as the saturating wavelength.

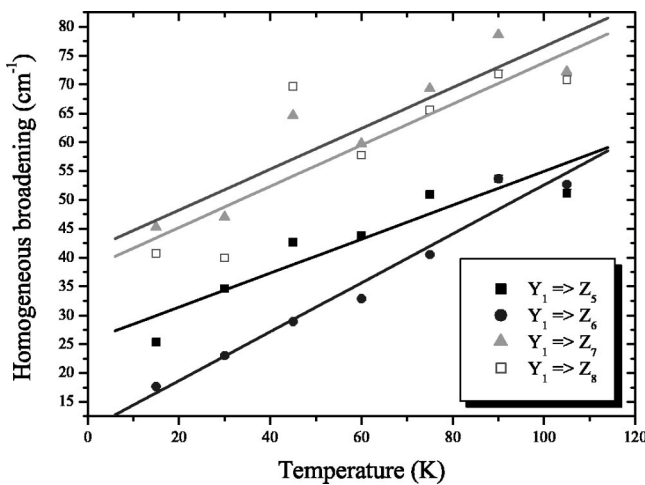


FIG. 9. Temperature dependence of the homogeneous broadening of the transition between the bottom Stark level of the  $^4I_{13/2}$  manifold and the upper Stark levels of the  $^4I_{15/2}$  manifold in the case of the fluoride sample. The points are the experimental measured linewidths and the lines result from a linear fit describing a one-phonon process.

This result confirms that the broadenings measured in this work can predict the impact of GSHB in the four tested matrices. Furthermore, our results explain why GSHB is so different in the *L* band (1570–1600 nm) compared to the *C* band (1530–1560 nm). Actually, in the *C* band, GSHB leads to well-defined and localized holes whereas in the *L* band, it manifests itself as a broadband gain depression.<sup>31</sup> Our results show that the transitions involved in the *L* band have large homogeneous linewidths compared to those involved in the *C* band. Therefore the *L* band has a homogeneous behavior in the saturating regime that leads to a broad depression over the entire homogeneous linewidth involved, whereas the *C* band exhibits an inhomogeneous behavior characterized by localized depression which manifests itself as a hole in the gain spectrum. Note that the homogeneous broadenings measured in this work are not equal to the hole FWHM obtained in GSHB. This can be due to the fact that, in GSHB experiments, the hole width is very sensitive to the saturating power.<sup>28,29</sup> It is observed that it increases as the saturating power increases.

## VI. CONCLUSION

This systematic study combines the direct measurement of the position and broadening of the energy levels of erbium



in four different glasses. A complete determination of the positions of the energy levels (Stark levels of the  $^4I_{15/2}$  and  $^4I_{13/2}$  manifolds) involved in the 1.55- $\mu\text{m}$  transition has been performed. It has also been possible to measure the inhomogeneous broadening and the homogeneous broadening of the zero-phonon transition and of some upper Stark levels within the  $^4I_{15/2}$  manifold; in this last case, the measurement was only possible for fluoride glass. The temperature dependence of the homogeneous broadening has also been studied and compared to a simplified theoretical law dominated by direct one-phonon and Raman processes.

The results obtained for the Stark splittings are in agreement with the conclusions of previous work and underline significant differences between the “symmetry” of the sites of the erbium ions, especially if we compare alkalisilicate glass to other glasses; it seems that the symmetry in these glasses is not as low as commonly supposed for rare-earth-doped glasses. This result has been confirmed by our inhomogeneous broadening measurement which is the smallest of the four tested glasses and is in agreement with the known role of alkaline ions. In the case of the other glasses, the large inhomogeneous broadening is probably related to a more rigid network or to a large variety of sites very similar from one ion to another. We observed larger homogeneous broadening in tellurite and fluoride compared to aluminosilicate and alkalisilicate. The temperature dependence for all

four glasses followed a  $T^{1.5}$  law, which suggests the combination of two broadening processes: a one-phonon process and a two-phonon Raman process. The comparison of the experimental results with a theoretical law involving those two processes was then performed. The fits underlined the relevance of the Debye temperature and hence of the phonon cutoff frequency in explaining the differences observed. The mechanisms involved in the broadening of the zero-phonon transition have also been found to be different from those for the upper Stark levels, for which only the one-phonon process seems to play a major role in the studied temperature range. It has also been possible to compare the broadenings measured in this work to those previously reported by other teams using GSHB approach. Even if differences exist on the value of the homogeneous broadening, the tendency is the same from one host to another and from one amplification band to another.

# ACKNOWLEDGMENTS

We are grateful to Pascal Baniel for fruitful discussions and to Bernard Varrel and Jean-Yves Rivoire for technical assistance. We show gratitude to Rufus L. Cone (MSU, Bozeman, U.S.) for a critical reading of the manuscript. This research was supported by Alcatel Research, Innovation Department, and CNRS.

\*Electronic address: bigot@pcml.univ-lyon1.fr

<sup>1</sup>E. Desurvire, *EDFA Principles and Applications* (Wiley, New York, 1994).

<sup>2</sup>Alcatel Research and Innovation Department website (2001).

<sup>3</sup>T. Komukai, T. Yamamoto, T. Sugawa, and Y. Miyajima, *Electron. Lett.* **29**, 100 (1993).

<sup>4</sup>F. Roy, A. Le Sauze, P. Baniel, and D. Bayart, in *Proceedings of Optical Amplifiers and their Applications, Stresa, 2001*, edited by N. Jolley, J. D. Minelly, and Y. Nakano, p. 24.

<sup>5</sup>S. Bigo *et al.*, in *Proceedings of Optical Fiber Conference, Anaheim, 2001*, edited by A. A. Sawchuk, p. PD-25.

<sup>6</sup>D. E. Goforth *et al.*, in *Proceedings of Optical Amplifiers and their Applications, Quebec, 2000*, edited by A. Mecozzi, M. Shimizu, and J. Zyskind, p. 159.

<sup>7</sup>S. Zemon, G. Lambert, W. J. Miniscalco, and B. A. Thompson, in *Proceedings of Fiber Laser Sources and Amplifiers III, Boston, 1991*, Vol. 1581, p. 91.

<sup>8</sup>S. C. Guy, R. A. Minasian, S. B. Poole, and M. G. Sceats, in *Proceedings of Optical Fiber Conference, San Diego, 1991*, p. FA2.

<sup>9</sup>J. L. Zyskind, E. Desurvire, J. W. Sulhoff, and D. J. Di Giovanni, *IEEE Photonics Technol. Lett.* **2**, 869 (1990).

<sup>10</sup>E. Desurvire, J. L. Zyskind, and J. R. Simpson, *IEEE Photonics Technol. Lett.* **2**, 246 (1990).

<sup>11</sup>A. Jha, S. Shen, and M. Naftaly, *Phys. Rev. B* **62**, 6215 (2000).

<sup>12</sup>C. C. Robinson, *J. Non-Cryst. Solids* **15**, 1 (1974).

<sup>13</sup>N. E. Alekseev *et al.*, in *Laser Phosphate Glasses*, edited by M. E. Zhabotinskii (Nauka, Moscow, 1980).

<sup>14</sup>S. Zemon, G. Lambert, W. J. Miniscalco, and B. A. Thompson, *J. Appl. Phys.* **69**, 6799 (1991).

<sup>15</sup>E. Desurvire and J. R. Simpson, *Opt. Lett.* **15**, 547 (1990).

<sup>16</sup>Y. D. Huang, M. Mortier, and F. Auzel, *Opt. Mater.* **15**, 243 (2001).

<sup>17</sup>Y. D. Huang, M. Mortier, and F. Auzel, *Opt. Mater.* **17**, 501 (2001).

<sup>18</sup>C. Brecher and L. A. Riseberg, *Phys. Rev. B* **13**, 81 (1976).

<sup>19</sup>B. Di Bartolo, in *Optical Interactions in Solids* (Wiley, New York, 1968), Vol. 15, p. 352.

<sup>20</sup>A. Ellens, H. Andres, A. Meijerink, and G. Blasse, *Phys. Rev. B* **55**, 173 (1997).

<sup>21</sup>R. M. MacFarlane and R. M. Shelby, in *Spectroscopy of Solids Containing Rare Earth Ions*, edited by A. A. Kaplyanskii and R. M. MacFarlane (North-Holland, Amsterdam, 1987), Vol. 3, p. 51.

<sup>22</sup>T. Kushida and E. Takushi, *Phys. Rev. B* **12**, 824 (1975).

<sup>23</sup>D. Bayart, B. Clesca, L. Hamon, and J. L. Beylat, *IEEE Photonics Technol. Lett.* **6**, 613 (1994).

<sup>24</sup>W. J. Miniscalco, *J. Lightwave Technol.* **9**, 234 (1987).

<sup>25</sup>R. M. MacFarlane and R. M. Shelby, *J. Lumin.* **36**, 179 (1987).

<sup>26</sup>X. Chen and B. Di Bartolo, *J. Lumin.* **54**, 309 (1993).

<sup>27</sup>D. K. Sardar and R. M. Yow, *Opt. Mater.* **14**, (2000).

<sup>28</sup>J. W. Sulhoff *et al.*, *IEEE Photonics Technol. Lett.* **9**, 1578 (1997).

<sup>29</sup>I. Joindot and F. Dupré, *Electron. Lett.* **33**, 1239 (1997).

<sup>30</sup>A. Yariv, in *Quantum Electronics* (John Wiley and Sons, New York, 1975), Vol. 8, p. 167.

<sup>31</sup>F. A. Flood, *IEEE Photonics Technol. Lett.* **12**, 1156 (2000).